Combinatorial Chemistry & High Throughput Screening, **2015**, *18*, **269-280**

A Ligand-Based Virtual Screening Approach to Identify Small Molecules as hERG Channel Activators

Elisa Giacomini[1,2,§], Rosa Buonfiglio[1,§,‡], Matteo Masetti[1], Yuhong Wang[3], Gea-Ny Tseng[3], Marinella Roberti[*,1] and Maurizio Recanatini[1]

[1]*Department of Pharmacy and Biotechnology, Alma Mater Studiorum - Università di Bologna, via Belmeloro 6, 40126 Bologna, Italy*

[2]*D3 Computation, Istituto Italiano di Tecnologia, via Morego 30, 16163 Genova, Italy*

[3]*Department of Physiology & Biophysics, Virginia Commonwealth University, Richmond, VA 23298, USA*

Marinella Roberti

Abstract: The hERG potassium channel is currently emerging as a potential target for the treatment of some forms of arrhythmias or to contrast an unintentional channel block caused by drugs. Despite its therapeutic relevance, so far only few compounds are described as able to enhance channel function by potentiating hERG currents. This gap is also related to the lack of hERG crystal structure which strongly limits the possibility to employ structure-based techniques in the search and design of novel activators. To overcome this limitation, in the present work, a ligand-based virtual screening was performed using as separate search queries two conformations of NS1643, the most deeply investigated and better characterized hERG activator. The library of compounds resulting from the virtual screening was then clustered based on recurring chemical features, and 5 hits were selected to be evaluated for their ability to enhance hERG current *in vitro*. Compound **3** showed a good activating effect, also displaying a mechanism of action similar to that of NS1643. Moreover, the most interesting compounds were further investigated by synthesizing in a parallel fashion some analogs, with the aim to get insights about structure-activity relationships.

Keywords: Activators, electrophysiology, hERG potassium channel, ligand-based virtual screening, NS1643, parallel synthesis.

INTRODUCTION

Ion channels are transmembrane proteins responsible for the passive and selective transport of ions through biological membranes, and thereby they contribute to regulate the excitability and osmotic equilibrium of living cells [1, 2]. These proteins are widely distributed all over the human body, and they are involved in several processes, such as transmission of nerve impulses, muscle contraction and relaxation, cognition, as well as in many other aspects of physiology [1]. The key role played by ion channels in the organism is mirrored by the large number of known diseases associated to their malfunctioning, which makes them attractive targets in the drug discovery field [3]. Among the others, the hERG potassium channel (Kv11.1) has aroused considerable scientific interest due to its relevant physiological function in the heart and its implication in arrhythmias.

*Address correspondence to this author at the Department of Pharmacy and Biotechnology, Alma Mater Studiorum - Università di Bologna, via Belmeloro 6, 40126 Bologna, Italy; Tel: +(39) 051 2099738;
E-mail: marinella.roberti@unibo.it

[§]These authors contributed equally to this work.

[‡]Present address: Computational Chemistry, Chemistry Innovation Centre, Discovery Sciences. AstraZeneca R&D Mölndal, SE-43183 Mölndal, Sweden.

The hERG-K^+ channel belongs to the voltage-gated family of potassium channels (Kv), and therefore it shows typical structural features shared by all members of this family, *i.e.* the tetrameric assembly of six transmembrane helices around the pore axis, the voltage sensing domain (helices S1 - S4), and the pore forming domain (helices S5 - S6) [4-6]. Along with these similarities, hERG shows several peculiarities of its own that appear to be responsible for the promiscuous drugs interactions [7, 8] or correlated to trafficking defects [9]. However, the most distinctive feature of the channel relies on its unique gating properties, characterized by slow activation and deactivation kinetics in opposition to a very fast voltage-dependent inactivation. These unusual kinetics find an explanation in the main role played by hERG in the ventricular cardiac action potential (AP) and refractoriness of cardiac cells. In cardiomyocytes, the channel slowly opens when the membrane starts to depolarize from the holding potential of -80 mV to more positive values, but once a value of -40 mV is reached, it rapidly enters in the inactivated state. It is only during late phase 2 of the AP that hERG quickly recovers from inactivation causing the typical large tail currents that significantly contribute to the membrane repolarization. Since these currents reach their maximum amplitude during phase 3 of the AP, they are properly referred to as rapidly activating delayed rectifier currents (IKr) [10].

Given the description above, it is clear that alterations of hERG channel function, either due to genetic mutations or

1875-5402/15 $58.00+.00

drug modulation, could lead to serious health conditions [11]. Notably, the most important and investigated correlation between the channel dysfunction and a cardiac pathology, regards the Long QT Syndrome (LQTS) [12]. LQTS is caused by an abnormal repolarization phase of the ventricular AP that is diagnosed by a marked prolongation of the QT interval of the electrocardiogram. People affected by this condition are predisposed to a rare but potentially fatal form of ventricular tachyarrhythmia named *torsades de pointes* (TdP) [13]. The unintentional hERG blockade by drugs is the major cause for the acquired LQTS, and over the past decades many drugs have been withdrawn from the market because of this unwanted effect [14]. In this scenario, hERG has always been traditionally considered as an antitarget, and many efforts have been undertaken in helping to identify potential blockers at the early stages of a drug design process with both *in vitro* and *in silico* methods [15,16]. The concept to consider hERG as a therapeutic target started to take place only in the past decade [17]. Indeed, compounds able to enhance channel function by potentiating hERG activity would accelerate the repolarization and shorten the duration of the AP [5], and such activators might become useful therapeutics to treat some forms of arrhythmias or simply to contrast the effect of the channel block. Despite their unquestionable therapeutic potential, only few compounds able to enhance IKr currents have been described so far, and for this reason there is a compelling need to search for more potent and/or diverse activators. By screening a large compound library of previously collected electrophysiology data, Zhang and coworkers have recently discovered a remarkably potent and effective hERG activator [18]. Without disregarding the impressive result, the drawback of this approach is either the requirement of prior knowledge, or the cost needed to build a new library from scratch. A well-established alternative comes from virtual screening (VS) approaches, which have long been used as valuable tools to screen libraries of up to millions of compounds in an effective and relatively inexpensive way. Here, we investigate the possibility to discover novel hERG modulators by means of such computational strategies.

Based on the current knowledge, hERG activators can enhance IKr currents with different mechanisms of action, and they have been retrospectively classified as type 1 and type 2 [4]. Both of them attenuate inactivation, but while type 1 activators severely slow deactivation, supposedly by binding on the pore domain of the channel, type 2 activators do not strongly affect deactivation properties, as they primarily act by shifting the voltage dependence of inactivation to more positive potentials. 1,3-Bis-(2-hydroxy-5-trifluoromethyl-phenyl)-urea (NS1643, see Table **1**) [19, 20] is considered as one of the most important and thoroughly examined type 2 activators [21]. It affects hERG in a concentration-dependent manner working from the extracellular side of the cell membrane, and its enhancing effect also involves a slowing of hERG inactivation, as well as an acceleration of channel activation and slowed deactivation. The location of the NS1643 binding site in the channel is still under debate [22, 23], and the possibility of multiple binding sites triggering diverse pharmacological effects has also been reported [20, 22, 23]. These uncertainties, together with the lack of the hERG crystal structure, do severely hamper a reliable VS strategy based on the knowledge of the three-dimensional structure of the target. To overcome this limitation, we performed a ligand-based VS (LBVS) of the Enamine vendor catalog [24] using two conformations of the NS1643 activator as search queries (Fig. **1A**). Then, the most interesting hits among the final library were purchased, and some of them were identified as moderate activators of the hERG-K^+ channel. Structure-activity relationships (SAR) were also undertaken with the aim to rationalize the effects of substituents on the enhancing effect of IKr currents.

MATERIALS AND METHODS

Ligand-Based Virtual Screening

The LBVS was performed using the workflow outlined in Fig. (**1B**). All the operations hereafter detailed were performed using programs belonging to the Openeye Scientific Software toolkit [25] unless otherwise stated.

NS1643, an effective type 2 hERG activator showing a maximal increase in currents amplitude of more than 300% at the concentration of 30 μM, and an apparent Kd value of 20 μM [7], was used as a query for the LBVS. Since the screening was performed so as to match the 3D chemical features of a reference compound (see below), it is of pivotal importance to represent the query molecule in its bioactive conformation [26]. However, in the absence of such an information, the *syn* and *anti* conformations of NS1643 were considered for the screening (Fig. **1A**). Both conformations were built and optimized with the Gaussian03 program package [27]. The B3LYP functional was used together with the split-valence 6-31G(d) basis set. The resulting structures were used as separate search queries in the step 2 and 3 of the LBVS.

Step 1. Drug-likeness and scaffold filtering. The Enamine vendor catalog [24], consisting of more than 10^6 compounds, was downloaded from the ZINC database [28] and used as compound library. The library was then filtered with the FILTER program [29], in order to discard non-drug like compounds and at the same time to focus the database towards desired knowledge-based derived chemical properties.

The molecular weight (MW), the number of rotatable bonds (NRB), the octanol-water partition coefficient (logP, calculated through the XlogP algorithm) [30], and the 2D polar surface area (2D-PSA) were chosen as basic physico-chemical descriptors to be used in the filtering. These quantities were calculated with the Molprop tool for a set of six known hERG activators (including NS1643, see Table **1**), and the upper and lower intervals of the filter were tuned so as to include approximately one standard deviation from the mean for each descriptor. Thus, the filter parameters were set to: MW = 300 - 500 Da, NRB = 2 - 7, logP = 2.4 - 5.4, and 2D-PSA = 37 - 110 $Å^2$. Besides these properties, the library was also filtered in order to exclude specific chemical groups. Reactive or labile groups, toxic groups, and protecting groups were limited or removed from the database, in order to minimize the chance to incur in false positives and false negatives. Thus, we discarded entries containing groups such as quinone, triflate, phosphoramide,

Table 1. Known hERG channel activators with the corresponding molecular descriptors used in step 1 of the LBVS protocol.

Activators	MW (Da)	NRB	logP	PSA (A^2)
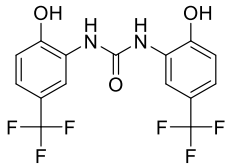 **NS1643**	380.06	6	2.718	81.59
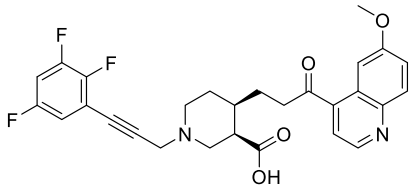 **RPR260243**	509.17	7	4.398	79.73
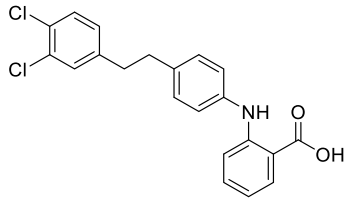 **PD118057**	384.06	6	5.104	49.33
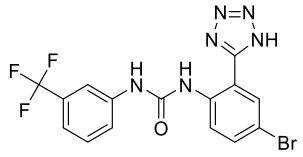 **NS3623**	426.01	6	3.784	95.59
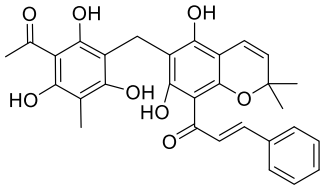 **Mallotoxin**	399.09	6	2.919	144.52
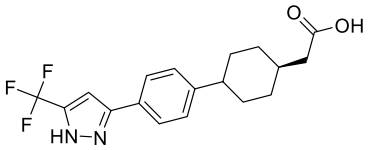 **A935142**	351.13	5	3.771	65.98

isonitriles, sulfonylnitriles, aldehydes, azides, azocompounds, peroxides. Default values as implemented in FILTER program were used. Moreover, dyes were not considered eligible because of non-specific binding to proteins. Finally, some functional groups were allowed in moderate quantity, including hydroxyls (no more than 6), olefins (no more than 4), and amides (no more than 4). After applying this filter, the total number of structures decreased to about 600.000 entries.

Since the following steps of the LBVS procedure relied on similarity searches based on comparison of 3D chemical features, a conformational analysis was performed with the OMEGA software [31]. To minimize the risk of discarding potentially interesting conformations, we used the default OMEGA settings of an energy window of 10 kcal mol^{-1} above the global minimum [32-34]. As a tradeoff between this requirement and computational efficiency, 50 conformers were generated for each compound, with a resolution of the conformational search of 1 Å measured on the heavy atoms RMSD.

Step 2. Shape-based similarity search. The shape similarity was evaluated with the Rapid Overlay of Chemical

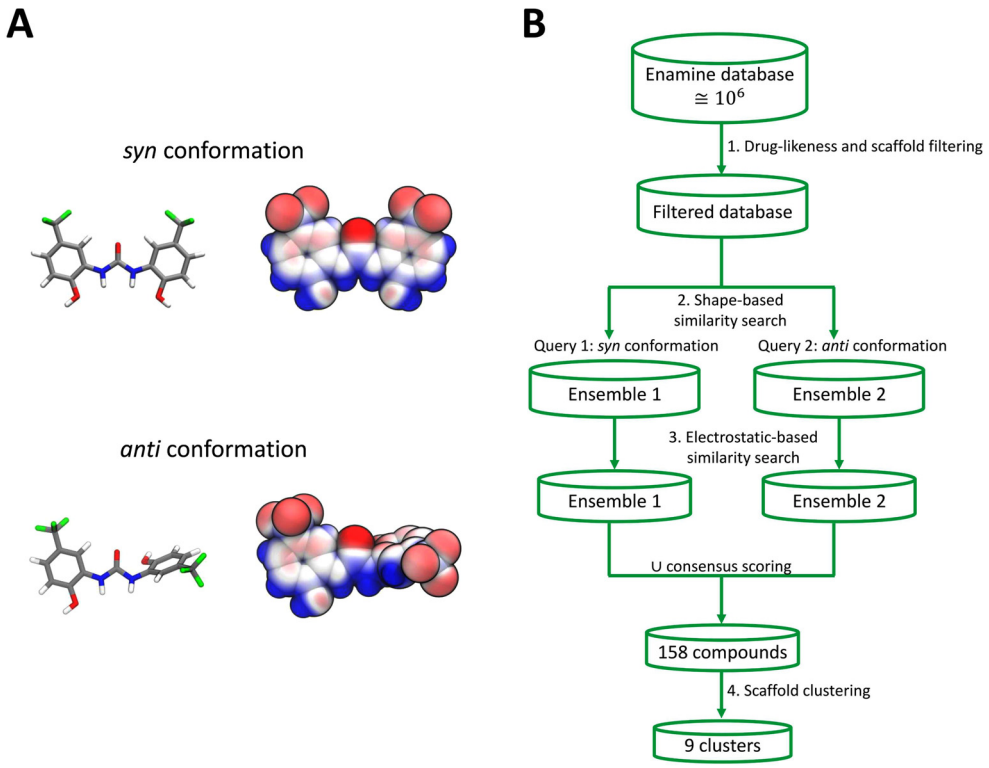

Fig. (1). (**A**) Graphical representation of the *syn* and *anti* conformations of NS1643 employed as search queries for the LBVS. On the left, the conformers are shown in sticks and the atoms are colored according to their atomic number, whereas on the right, the molecules are represented as van der Waals spheres colored according to the *ab initio* electrostatic potential (red to blue for more negative and more positive values, respectively). (**B**) The LBVS workflow.

Structures (ROCS) software [35, 36], which aligns molecules by optimizing the overlap between their volumes. The Tanimoto Combo was used as a metric to score and rank the overlaps. After a preliminary visual inspection, a cutoff of 0.8 was found as the optimal threshold to filter out database molecules with a low shape overlap, and was employed to prune the library. All the other parameters were set to default values. The conformations were processed with ROCS as unique entries and stored in the output hits file based on their individual shape overlay. The 3D structures of the *syn* and *anti* conformations of NS1643 were separately used as reference structures for two parallel screenings.

Step 3. Electrostatic-based similarity search. The electrostatic similarity was evaluated with EON [37] by comparing the electrostatic potential map of the molecules in their relative orientation as obtained by ROCS in the previous step. The MMFF94 [38] force field was used to calculate partial charges for the compounds of the library, whereas RESP charges [39, 40] calculated at the B3LYP/6-31G(d)//B3LYP/6-31G(d) level of theory with the Gaussian03 package [27] were used for the query molecule in both conformations. The electrostatic potential of the *syn* and *anti* conformations of NS1643 is shown in Fig. (**1A**). For the calculation of partial charges, all the molecules were considered in the most populated protonation state at neutral pH. The Electrostatic Tanimoto Combo was used to assess the electrostatic similarity, and the 1000 top ranked compounds were stored applying a cutoff value of 1.22. Similarly to the previous step, the electrostatic maps of the *syn* and *anti* conformers were used independently to screen the database.

Step 4. Scaffold clustering. Among the two ensembles of screened molecules, only entries satisfying simultaneously the 3D features of the *syn* and *anti* conformations were further considered (consensus scoring). This allowed us to reduce the database to a number of 158 molecules. Since all molecules consisted of a pair of diversely substituted aromatic rings separated by recurring spacers, we decided to cluster the library based on the chemical features of this central portion. A hierarchical clustering algorithm was used, as implemented in the ICM software [41]. In particular, the tree is built using the UPGMA (Unweighted Pair Group Method Using Arithmetic Average) algorithm, based on sequential clustering of the smallest pairwise distance in the Tanimoto distance matrix of the molecules [42]. In Table **2**, the chemical structures of the 9 clusters are reported. Five molecules, that is the 3% of this library, were finally selected to be tested for their ability to enhance hERG currents.

Chemistry

General Chemical Methods. Reaction progress was monitored by TLC on pre-coated silica gel plates (Kieselgel 60 F_{254}, Merck) and visualized by UV254 light. Compounds **1-5** (Table **3**) were purchased by Enamine, while compounds **6-16** (Table **3**) were synthesized as shown in Scheme **1**. All reagents were purchased from Aldrich and were of analytical grade, so they were used without further purification. All

Table 2. The nine scaffold clusters identified for the 158 molecules. R and R_1 are substituted aromatic rings such as benzene, pyridine, thiophene, furane, or fused rings variously substituted.

Scaffold 1 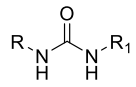	Scaffold 2 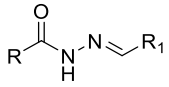	Scaffold 3 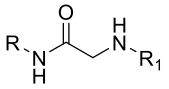
Scaffold 4 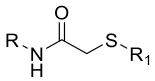	Scaffold 5 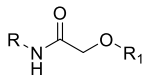	Scaffold 6 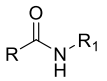
Scaffold 7 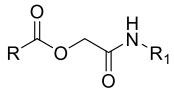	Scaffold 8 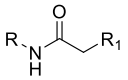	Scaffold 9 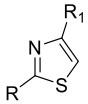

solvents were distilled prior to use. All reactions were carried out under an inert atmosphere. Compounds were named relying on the naming algorithm developed by CambridgeSoft Corporation and used in Chem-BioDraw Ultra 13.0. ^{1}H-NMR and ^{13}C-NMR spectra were recorded on Varian Gemini at 400 MHz and 100 MHz respectively. Chemical shifts (δ_H) are reported relative to TMS as internal standard. IR-FT spectra were performed in Nujol and obtained on a Nicolet Avatar 320 E.S.P. instrument; ν value max is expressed in cm-1. Mass spectrum was recorded on a V.G. 7070E spectrometer or on a Waters ZQ 4000 apparatus operating in electrospray (ES) mode.

General Parallel Procedure for the Synthesis of Amides 1, 4, 8-12

In distinct reactors, carboxylic acids (1 equiv) **17**-**21**, 1-hydroxybenzotriazole (1.2 equiv), and suitable amines **22-24** (1.2 equiv), were dissolved in dimethylformamide at room temperature. DCC (1.2 equiv) was added, and the mixtures were stirred at room temperature overnight. The precipitate of dicyclohexylurea was filtered off and the filtrate was added in cold stirring water and extracted with ethyl acetate x 3. The combined organic layers were dried over Na_2SO_4 and evaporated under reduced pressure. Each crude product was purified by flash chromatography on a short pad of silica gel.

General Procedure to Obtain Hydroxy Amides 6, 7, 13-16

In distinct round bottom flasks, to a stirring solution of amides (1 equiv) **1**, **4**, **8-12** in dry dichloromethane, BBr_3 1 M was added dropwise (1 equiv for each methoxy group) under an inert atmosphere at -72 °C. The resulting mixtures were stirred at room temperature for 20 h. Afterwards, the reaction was quenched with water, and the aqueous phase extracted with dichloromethane x 2. The combined organic layers were dried over Na_2SO_4 and evaporated under reduced pressure. Each crude product was purified by flash chromatography on a short pad of silica gel.

N-(2,5-Dimethoxyphenyl)-2-(Phenylthio)Acetamide 1

2-(Phenylthio)acetic acid **17** (0.30 g, 1.78 mmol), 2,5-dimethoxyaniline **22** (0.32 g, 2.14 mmol) were allowed to react according to the described general procedure and the crude product was purified on silica eluting with petroleum ether and ethyl acetate 9.3:0.7. **1**: 0.34 g (yield 63 %); brown solid. ^{1}H-NMR (400 MHz, $CDCl_3$) δ 3.75 (s, 3H), 3.76 (s, 2H), 3.77 (s, 3H), 6.56 (dd *J*= 8.8, 2.8 Hz, 1H), 6.76 (d, *J*= 8.8 Hz, 1H), 7.18-7.22 (m, 1H), 7.26-7.30 (m 2H), 7.37-7.39 (m, 2H), 8.04 (d, *J*= 3.2 Hz, 1H), 9.22 (br, 1H) ppm. ^{13}C-NMR (100 MHz, $CDCl_3$) δ 38.6, 55.1, 55.7, 105.2, 108.3, 110.4, 126.4, 127.2, 128.5, 128.7, 133.6, 141.9, 153.2, 165.3 ppm. MS (ES): m/z 326 ($M + Na^+$).

N-(5-Chloro-2,4-Dimethoxyphenyl)-3a,7a-Dihydro-1H-Indazole-3-Carboxamide 4

1H-indazole-3-carboxylic acid **18** (0.30 g, 1.85 mmol), 5-chloro-2,4-dimethoxyaniline **23** (0.42 g, 2.22 mmol) were allowed to react according to the described general procedure and the crude product was washed with methanol, and filtered. **4**: 0.35 g (yield 43 %); white solid. ^{1}H-NMR (400 MHz, $(CD_3)_2CO$) δ 3.97 (s, 3H), 4.10 (s, 3H), 7.00(s, 1H), 7.36-7.40 (m, 1H), 7.50-7.55 (m, 1H), 7.74 (tt, *J*= 0.8, 8.4 Hz, 1H), 8.40-8.42 (m, 1H), 8.73 (s, 1H), 9.43 (br, 1H) ppm. ^{13}C-NMR (100 MHz, $(CD_3)_2CO$) δ 56.9, 57.0, 98.5, 111.6, 113.4, 121.0, 121.1, 122.5, 122.8, 122.8, 123.6, 127.9, 149.0, 149.1, 152.1, 160.8 ppm.

N-(5-Tert-Butyl-2-Methoxyphenyl)-2-(Phenylthio)Acetamide 8

2-(Phenylthio)acetic acid **17** (0.15 g, 0.89 mmol), 5-*tert*-butyl-2-methoxyaniline **24** (0.19 g, 1.07 mmol) were allowed to react according to the described general procedure and the crude product was placed on a short pad of silica gel and eluted with petroleum ether and ethyl acetate 9:1. **8**: 0.13 g (yield 45 %); white powder; ^{1}H-NMR (400 MHz, $CDCl_3$) δ 1.28 (s, 9H), 3.76 (s, 2H), 3.79 (s, 3H), 6.77 (d, *J*= 8 Hz, 1H), 7.03 (m, 1H), 7.21 (s, 1H), 7.20-7.30 (m 2H), 7.39 (dd, *J*= 8.4, 1.2 Hz, 2H), 8.41 (d, *J*= 2 Hz, 1H), 9.19 (br, 1H) ppm. ^{13}C-NMR (100 MHz, $CDCl_3$) δ 31.4, 34.4, 39.2, 55.8, 109.6, 117.2, 120.6, 126.7, 127.0, 129.2, 129.3, 134.4, 144.0, 146.2, 165.7 ppm.

Table 3. Percentage of activation on hERG current amplitude of synthesized compounds.

Compounds	I_d/I_c%	Compounds	I_d/I_c%
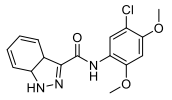 **4**	140%[a]	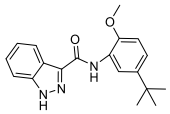 **9**	134%[c]
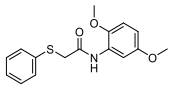 **1**	167%[a]	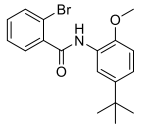 **10**	160%[c]
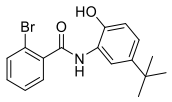 **3**	195%[a]	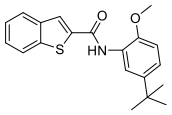 **11**	109%[c]
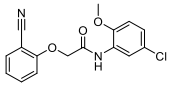 **2**	148%[a]	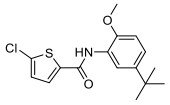 **12**	127%[c]
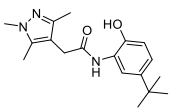 **5**	123%[a]	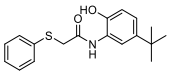 **13**	125%[c]
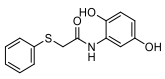 **6**	67%[b]	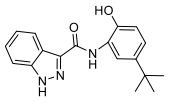 **14**	116%[c]
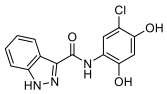 **7**	38%[a]	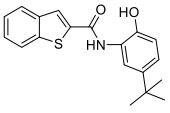 **15**	111%[c]
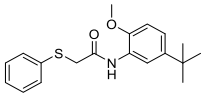 **8**	116%[c]	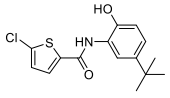 **16**	119%[c]

[a]Tested at 30μM; [b]tested at 100μM; [c]tested at 20μM.

N-(5-Tert-Butyl-2-Methoxyphenyl)-1H-Indazole-3-Carboxamide 9

1H-indazole-3-carboxylic acid **18** (0.20 g, 1.23 mmol), 5-*tert*-butyl-2-methoxyaniline **24** (0.27 g, 1.48 mmol) were allowed to react according to the described general procedure and the crude product was placed on a short pad of silica gel and eluted with petroleum ether and ethyl acetate 9:1. **9**: 0.30 g (yield 74 %); white powder; ^{1}H-NMR (400 MHz, $CDCl_3$) δ 1.35 (s, 9H), 3.92 (s, 3H), 6.85 (d, *J*= 8.4 Hz, 1H), 7.08 (m, 1H), 7.29-7.33 (m, 1H), 7.41-7.45 (m, 1H), 7.51-7.53 (m, 1H), 8.48-8.51 (m, 1H), 9.53 (br, 1H), 10.36 (br, 1H) ppm. ^{13}C-NMR (100 MHz, $CDCl_3$) δ 31.7, 34.6, 56.1, 109.6, 109.9, 117.4, 120.2, 122.2, 122.9, 123.1, 127.4, 127.6, 140.3, 141.6, 144.3, 146.3, 160.5 ppm.

2-Bromo-N-(5-Tert-Butyl-2-Methoxyphenyl)Benzamide 10

2-Bromobenzoic acid **19** (0.15 g, 0.75 mmol), 5-*tert*-butyl-2-methoxyaniline **24** (0.16 g, 0.89 mmol) were allowed to react according to the described general procedure and the crude product was placed on a short pad of silica gel and eluted with petroleum ether and ethyl acetate 9:1. **10**: 0.14 g (yield 45 %); red solid; ^{1}H-NMR (400 MHz, $CDCl_3$) δ 1.35 (s, 9H), 3.84 (s, 3H), 6.83 (d, *J*= 8.8 Hz, 1H), 7.10 (dd, *J*= 2.4, 8.4 Hz, 1H), 7.31 (dd, *J*= 8, 2 Hz, 1H), 7.37-7.41 (m, 1H), 7.62-7.66 (m, 2H), 8.29 (br, 1H), 8.64 (d, *J*= 2.4 1H) ppm. ^{13}C-NMR (100 MHz, $CDCl_3$)δ 31.5, 34.5, 55.8, 109.6, 117.4, 119.4, 120.7, 127.0, 127.6, 129.8, 131.4, 133.6, 138.3, 144.2, 146.0, 165.2 ppm.

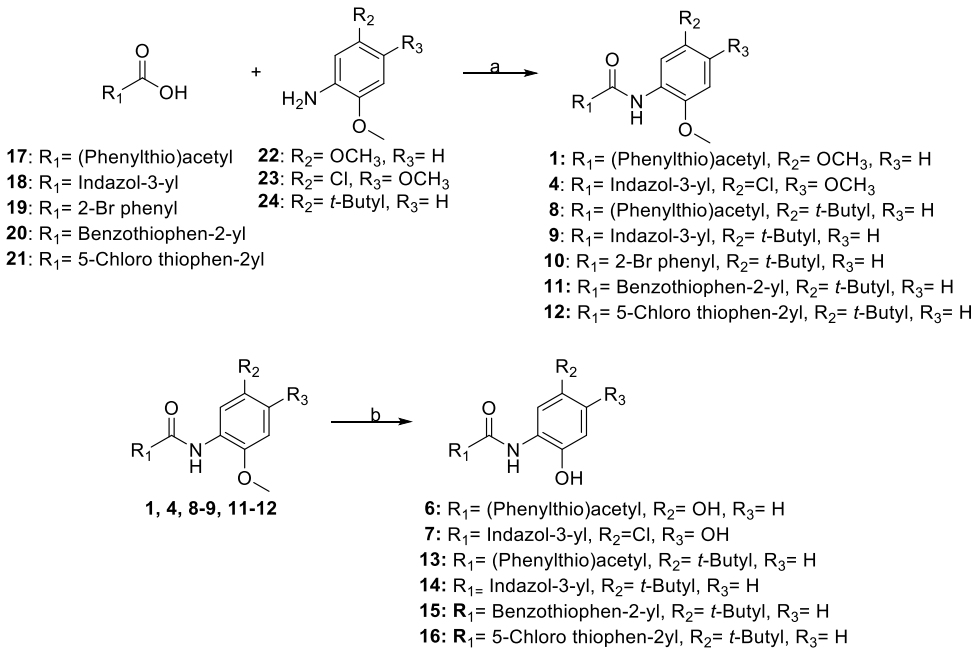

Scheme 1. Reagents and conditions: a) DCC, OHBt, DMF, 12h, room temp.; BBr_3 1M, CH_2Cl_2, 24h, -72° to room temp.

N-(5-Tert-Butyl-2-Methoxyphenyl)Benzothiophene-2-Carboxamide 11

Benzothiophene-2-carboxylic acid **20** (0.20 g, 1.12 mmol), 5-*tert*-butyl-2-methoxyaniline **24** (0.24 g, 1.35 mmol) were allowed to react according to the described general procedure and the crude product was placed on a short pad of silica gel and eluted with petroleum ether and ethyl acetate 9.9:0.1, then washed with petroleum ether. **11**: 0.25 g (yield 66 %); white powder; ^{1}H-NMR (400 MHz, $CDCl_3$) δ 1.34 (s, 9H), 3.93 (s, 3H), 6.85 (d, *J*= 8.8 Hz, 1H), 7.08-7.11 (m, 1H), 7.40-7.44 (m, 2H), 7.84 (1H), 7.86-7.88 (m, 2H), 8.54 (1H), 8.61 (d, *J*=2 1H) ppm. ^{13}C-NMR (100 MHz, $CDCl_3$) δ 31.5, 34.5, 55.9, 109.4, 117.4, 120.6, 122.7, 124.9, 125.0, 125.1, 126.4, 126.9, 139.2, 139.6, 141.2, 144.3, 145.8, 160 ppm.

N-(5-Tert-Butyl-2-Methoxyphenyl)-5-Chlorothiophene-2-Carboxamide 12

5-Chlorothiophene-2-carboxylic acid **21** (0.20 g, 1.23 mmol), 5-*tert*-butyl-2-methoxyaniline **24** (0.26 g, 1.48 mmol) were allowed to react according to the described general procedure and the crude product was placed on a short pad of silica gel and eluted with petroleum ether and ethyl acetate 9.9:0.1, then washed with petroleum ether. **12**: 0.23 g (yield 58 %); white powder; ^{1}H-NMR (400 MHz, $CDCl_3$) δ 1.31 (s, 9H), 3.89 (s, 3H), 6.82 (d, *J*= 8 Hz, 1H), 6.93 (d, *J*= 4.4 Hz, 1H), 7.07 (dd, *J*= 8.4, 2.4 Hz, 1H), 7.36 (d, *J*= 4.4 Hz, 1H), 8.28 (br, 1H), 8.51 (d, *J*= 2.4 Hz, 1H) ppm. ^{13}C-NMR (100 MHz, $CDCl_3$) δ 31.5, 34.4, 55.9, 109.4, 117.4, 120.5, 126.71, 127.1, 135.8, 138.6, 144.3, 145.7, 158.6 ppm.

N-(2,5-Dihydroxyphenyl)-2-(Phenylthio)Acetamide 6

To a stirring solution of amide (0.10 g, 0.33 mmol) **1** in dichloromethane dry was added dropwise BBr_3 1M (0.66 mL, 0.66 mmol, 2 equiv) according to the general procedure described above. The crude product was purified on silica eluting with dichloromethane and methanol 9.9:0.1.**6:** 0.06 g (yield 66 %); white powder; ^{1}H-NMR (400 MHz, $(CD_3)_2CO$) δ 3.91 (s, 2H), 6.41-6.44 (m, 1H), 6.70 (d, *J*= 8.8 Hz, 1H), 7.19-7.24 (m, 1H), 7.29-7.34 (m, 2H), 7.44-7.47 (m, 2H), 7.52 (d, *J*= 2.8 Hz, 1H), 7.78 (br, 1H), 8.33 (br, 1H), 9.29 (br, 1H) ppm. ^{13}C-NMR (100 MHz, $(CD_3)_2CO$) δ 38.9, 108.1, 111.5, 116.4, 127.3, 127.5, 129.8, 130, 135.7, 140.2, 150.9, 167.6 ppm. IR ν_{max} (Nujol) cm^{-1} 3321, 3117, 1649, 1604, 1555, 1460, 1375, 1258, 735, 689. MS (ES): m/z 298 (M + Na^+).

N-(5-Chloro-2,4-Dihydroxyphenyl)-3a,7a-Dihydro-1H-Indazole-3-Carboxamide 7

To a stirring solution of amide (0.10 g, 0.30 mmol) **4** in 5 mL of dichloromethane dry was added dropwise BBr_3 1M (0.60 mL, 0.60 mmol, 2 equiv) according to the general procedure described above. The crude product was purified on silica eluting with dichloromethane and methanol 9.9:0.1. **7**: 0.08 g (yield 66 %); white powder; ^{1}H-NMR (400 MHz, $(CD_3)_2CO$) δ 6.70 (s, 1H), 7.31-7.32 (m, 1H), 7.45-7.49 (m, 1H), 7.67-7.70 (m, 1H), 8.32 (d, *J*= 2.8, 1H), 8.34-8.37 (m, 1H), 9.51 (br, 1H) ppm. ^{13}C-NMR (100 MHz, $(CD_3)_2CO$) δ 104.9, 110.9, 111.6, 121.1, 121.7, 122.7, 122.7, 123.4, 127.8, 139.4, 142.8, 147.6, 150.3, 161.3 ppm. IR ν_{max} (Nujol) cm^{-1} 3469, 3364, 3222, 1651, 1546, 1514, 1462, 1376. MS (ES): m/z 326 (M + Na^+).

N-(5-Tert-Butyl-2-Hydroxyphenyl)-2-(Phenylthio)Acetamide 13

To a stirring solution of amide (0.17 g, 0.53 mmol) **8** in 4 mL of dry dichloromethane BBr_3 1M (0.53 mL, 0.53 mmol, 1 equiv) was added dropwise according to the general procedure described above. The crude product was placed on a short pad of silica gel and eluted with petroleum ether and ethyl acetate 9:1.**13**: 0.15 g (yield 89 %); white powder; ^{1}H-NMR (400 MHz, $CDCl_3$) δ 1.23 (s, 9H), 3.81 (s, 2H), 6.81 (d, *J*= 2.4 Hz, 1H), 6.92 (d, *J*= 8.4 Hz, 1H), 7.13 (dd, *J*= 8.4

2.4 Hz, 1H), 7.26-7.28 (m, 1H), 7.31-7.38 (m, 4H), 8.22 (br, 1H), 8.72 (br, 1H) ppm. ^{13}C-NMR (100 MHz, $CDCl_3$) δ 31.3, 33.9, 38.1, 118.9, 119.4, 124.1, 124.7, 127.5, 128.9, 129.6, 133.4, 143.7, 146.4, 168.1 ppm. IR ν_{max} (Nujol) cm^{-1} 3327, 2730, 1645, 1592, 1548, 1509, 1462, 1377, 1310, 1286, 1247, 1200, 1129, 822, 745, 721.

N-(5-Tert-Butyl-2-Hydroxyphenyl)-1H-Indazole-3-Carboxamide 14

To a stirring solution of amide (0.25 g, 0.77 mmol) **9** in 5 mL of dry dichloromethane BBr_3 1M (0.77 mL, 0.77 mmol, 1 equiv) was added dropwise according to the general procedure described above, and the crude product was placed on a short pad of silica gel and eluted with petroleum ether and ethyl acetate 8:2. **14**: 0.17 g (yield 71 %); white powder; ^{1}H-NMR (400 MHz, CD_3OD) δ 1.32 (s, 9H), 6.81 (d, *J*= 8.8 Hz, 1H), 6.99-7.01 (m, 1H), 7.27-7.30 (m, 1H), 7.43 (m, 1H), 7.59 (d, *J*= 8.4 Hz, 1H), 8.28-8.30 (m, 1H), 8.34 (d, *J*= 2.4 Hz, 1H) ppm. ^{13}C-NMR (100 MHz, CD_3OD) δ 32.0, 35.2, 110.6, 115.5, 118.8, 122.2, 122.7, 123.1, 123.7, 127.0, 128.0, 139.7, 143.2, 143.8, 145.8, 162.9 ppm.

N-(5-Tert-Butyl-2-Hydroxyphenyl)Benzo[b]Thiophene-2-Carboxamide 15

To a stirring solution of amide (0.30 g, 0.88 mmol) **11** in 5 mL of dry dichloromethane BBr_3 1M (0.88 mL, 0.88 mmol, 1 equiv) was added dropwise according to the general procedure described above. The crude product was placed on a short pad of silica gel and eluted with petroleum ether and ethyl acetate 9:1. **15**: 0.13 g (yield 45 %); white powder; ^{1}H-NMR (400 MHz, $CDCl_3$) δ 1.30 (s, 9H), 6.99 (d, *J*= 8.4 Hz, 1H), 7.21 (ddd, *J*= 7.2, 2.4 Hz, 2H), 7.42-7.50 (m, 2H), 7.88-7.89 (m, 1H), 7.90 (d, *J*=2.4 Hz, 1H), 7.97 (d, *J*= 8 Hz, 1H), 8.03 (s, 1H), 8.05 (s, 1H) ppm. ^{13}C-NMR (100 MHz, $CDCl_3$) δ 31.6, 34.3, 119.4, 119.5, 122.9, 124.6, 124.7, 125.4, 125.5, 127.1, 127.2, 136.9, 139.1, 141.5, 144.2, 146. 4, 161.8 ppm.

N-(5-Tert-Butyl-2-Hydroxyphenyl)-5-Chlorothiophene-2-Carboxamide 16

To a stirring solution of amide (0.30 g, 0.93 mmol) **12** in 5 mL of dry dichloromethane BBr_3 1M (0.93 mL, 0.93 mmol, 1 equiv) was added dropwise according to the general procedure described above. The crude product was placed on a short pad of silica gel and eluted with petroleum ether and ethyl acetate 9.5:0.5. **16**: 0.23 g (yield 80 %); white powder; ^{1}H-NMR (400 MHz, $CDCl_3$) δ 1.23 (s, 9H), 6.95-6.97 (m, 2H), 7.15-7.17 (m, 1H), 7.20 (d, *J*=2.4 Hz, 1H), 7.45 (d, *J*= 4 Hz, 1H), 7.84 (br, 2H) ppm. ^{13}C-NMR (100 MHz, $CDCl_3$) δ 31.4, 34.1, 119.0, 119.1, 124.3, 124.4, 127.3, 128.5, 136.0, 137.1, 144.0, 145.9, 160.0 ppm. IR ν_{max} (Nujol) cm^{-1} 3378, 1633, 1592, 1566, 1549, 1462, 1433, 1376.

Electrophysiology

Oocyte Expression, Two-Electrode Voltage Clamp and Data Analysis

Stage V oocytes were selected for expression. Each oocyte was injected with 40 nl solution containing 10 ng of hERG cRNA. After cRNA injection, oocytes were incubated in an ND96-based medium (ND96 supplemented with 4% horse serum, penicillin/streptomycin) for 2 - 4 days before experiments. During voltage clamp experiments, the oocyte was superfused with a low [Cl^-] ND96 solution (to minimize interference from endogenous Cl currents) at room temperature with whole oocyte currents recorded using the double-microelectrode recording configuration and OC-725C (Warner Instruments, MA) or GeneClamp 500 (Molecular Devices) amplifier. Voltage clamp protocol generation and data acquisition were controlled by pClamp 10 *via* DigiData 1440A (Molecular Devices). Current data were low-pass filtered at 1 kHz (Frequency Devices, MA) and stored on disks for off-line analysis. The following software was used for data analysis: pClamp 10, EXCEL (Microsoft), SigmaPlot, SigmaStat, and PeakFit (SPSS).

RESULTS AND DISCUSSION

The Enamine database, consisting initially of more than 10^6 compounds, was virtually screened in search for potential hERG activators, leading to a library of 158 molecules. Since the crystal structure of the hERG channel is at present not available, a structure-based VS could not have been safely performed for two entwined reasons. First, even though several homology models of the channel have been reported over the years [23, 43, 44], the percentage of identity between hERG and the currently available templates is in general too low to allow a reasonable chance of success in a VS campaign. Indeed, it is well known that the performance of structure-based VS is strongly dependent on the quality of the geometry of the target, and in this case the picture is worsened by the fact that some activators have been hypothesized to bind to the so-called "turret" of the channel. This portion is a distinctive feature of hERG [44], and in order to model it, one would face the challenging issue of building a 40 aminoacids segment from scratch, leading to the possibility to obtain an arguably reliable geometry. The second motivation that prompted us to employ a ligand-based VS, was the current uncertainty concerning the location of the NS1643 binding site. While some of us reported the pore entrance at the outer mouth of the selectivity filter as a possible binding site [7], the S5-S6 segment of two adjacent subunits of the channel in proximity of the pore helix has also been advanced to be implicated in binding [21]. Recently, through an ingenious topographic mapping of a homology modeling derived structure, Durdagi and coworkers have shown that the NS1643 binding to the channel appears to be extremely complex, and that the presence of multiple binding sites cannot be excluded [23]. In light of these considerations, we decided to embark on a LBVS based on the 3D chemical features of NS1643, which was one of the most potent and effective activators at the time this study was started. Two conformations of NS1643 were therefore considered during the screening, the *syn* and the *anti* conformations.

The 158 molecules library generated through the LBVS procedure, was carefully examined by visual inspection, and, since the repeating feature was the presence of two diversely decorated aromatic rings separated by recurring spacers, we decided to cluster it according to the functional groups of the linker itself. In Table **2**, the 9 obtained clusters are reported. Molecules belonging to Scaffold 1 were discarded because of their high similarity with known hERG activators.

Similarly, we decided not to take into consideration Scaffold 2 as the electrostatic potential map of the corresponding molecules did not satisfactorily match the one displayed by NS1643 in both the *syn* or *anti* conformations. Among the remaining clusters, only scaffolds 4-6, and 8 were considered, as they could allow SAR studies to be conducted taking advantage of a combinatorial approach. The molecules to be tested *in vitro* were therefore selected on the basis of their LBVS ranking depending on their commercial availability, and are shown in Table **3**. Specifically, a phenylthio acetamide derivative (**1**) was selected from Scaffold 4, a phenoxy acetamide (**2**) from Scaffold 5; Scaffold 6 represented the most populated cluster, therefore amides **3** and **4**, bearing diverse aromatic groups, were chosen from this ensemble. Finally, an acetamide derivative (**5**) was selected from Scaffold 8.

Preliminary assays on molecules **1**-**5** (Table **3**) involved the evaluation of the increment of the current amplitude measured before and after drugs application (30 μM) on wt hERG expressed in oocytes. Channel activation was performed starting from a holding potential of -80 mV, and depolarizing up to 60 mV with voltage steps of 20 mV. The currents were measured at the peak of the bell-shaped test pulse current-voltage relation, most often at 0 mV. We chose this physiologically relevant parameter because this is almost the plateau voltage of cardiac action potential, where IKr matters the most. Among the tested compounds, **3** showed the best result, increasing the current amplitude of 195%. Notably, as shown in Fig. (**2**), **3** is effective in increasing outward currents through the hERG/I_{Kr} channel during the plateau phase of cardiac action potential (Fig. **2C**), and this is likely due to a decrease in the degree of hERG/IKr inactivation (Fig. **2E**). However, **3** does not affect the voltage-dependence of hERG/I_{Kr} activation (Fig. **2D**) or the pore conductance of the hERG/I_{Kr} channel ($I_{fully\text{-}activated}$ at -120 mV). This behavior suggested that its mechanism could be similar to that of NS1643.

Unfortunately, the poor solubility of the other selected compounds made their evaluation quite difficult, especially for **2**. However, we determined that **1** increased current amplitude of 167%, **4** had a modest effect (140%), while **5** did not significantly enhance the currents.

From the above reported results, compound **3** appeared to be an interesting scaffold worth of further investigation, whereas the need of more soluble compounds came up to be a serious issue. With the aim to rationalize our findings with structure-activity relationships, and at the same time to obtain more soluble analogs, we decided then to pursue two roads. On one side, we explored the chemical space around **3** by keeping the 2-hydroxy-5-(*tert*-butyl)-aniline fragment resembling the 2-hydroxy-5-trifluoromethyl-phenyl of NS1643, and coupling it with different carboxylic acids

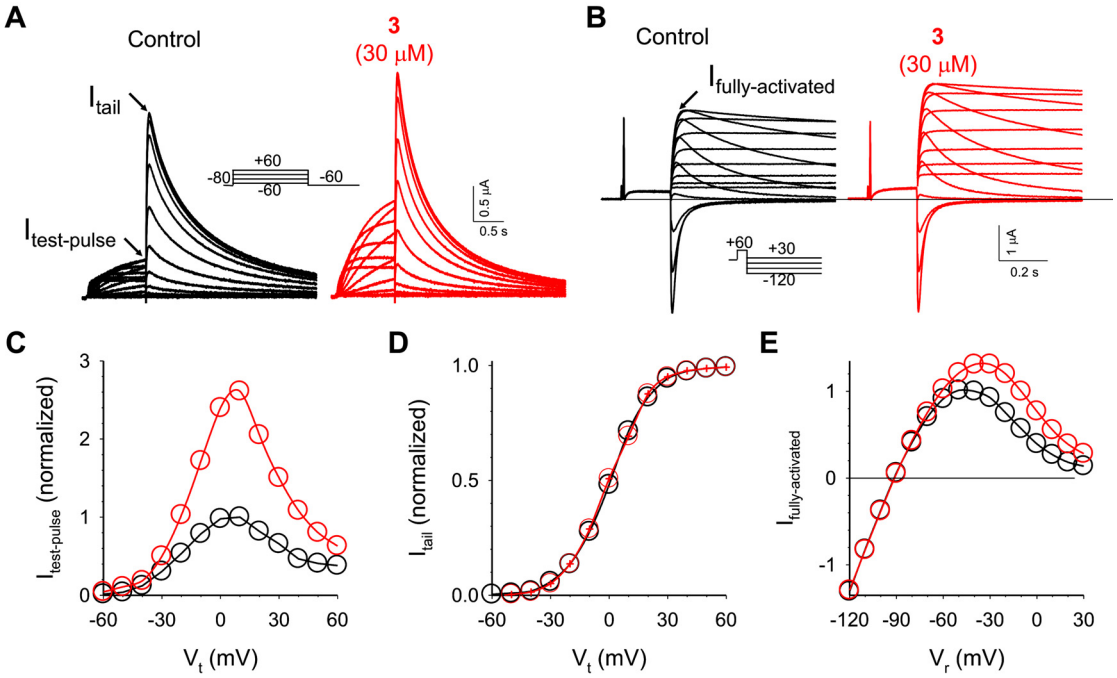

Fig. (2). Illustration of how hERG current amplitude and gating kinetics are quantified and the effects of compound 3. In all 5 panels, current traces or data points shown in black are control and those shown in red represent steady-state effects of **3** at a concentration of 30 μM. (**A**) Current traces elicited by the diagrammed voltage clamp protocol. The current amplitudes measured at the end of the test pulses ($I_{test\text{-}pulse}$) and the peak of the tail currents (I_{tail}) are noted. The values of $I_{test\text{-}pulse}$ are plotted against test pulse voltage (V_t) in (**B**); this parameter mimics the hERG/I_{Kr} current amplitudes during the cardiac action potential plateau phase. The values of I_{tail} are plotted against V_t in (**C**); the relationship between I_{tail} and V_t reflects the voltage-dependence of hERG/I_{Kr} activation. (**D**) Current trances elicited by the diagrammed voltage clamp protocol. The peak or plateau phase of the tail current is marked as $I_{fully\text{-}activated}$. The values of $I_{fully\text{-}activated}$ are plotted against repolarization voltage (V_r) in (**E**); this I-V relationship is a measure of the degree and voltage-dependence of hERG/I_{Kr} inactivation, seen here as a voltage-dependent decrease in current amplitude $\geq$ -30 mV. The amplitudes of inward currents seen at hyperpolarized voltages (*e.g.* -120 mV) indicate whether the pore conductance is altered. Statistical analysis: $I_{test\text{-}pulse}$ in the presence of compound 3 is significantly higher than that of control in the Vt range -20 to +50 mV (t-test, $p < 0.05$).

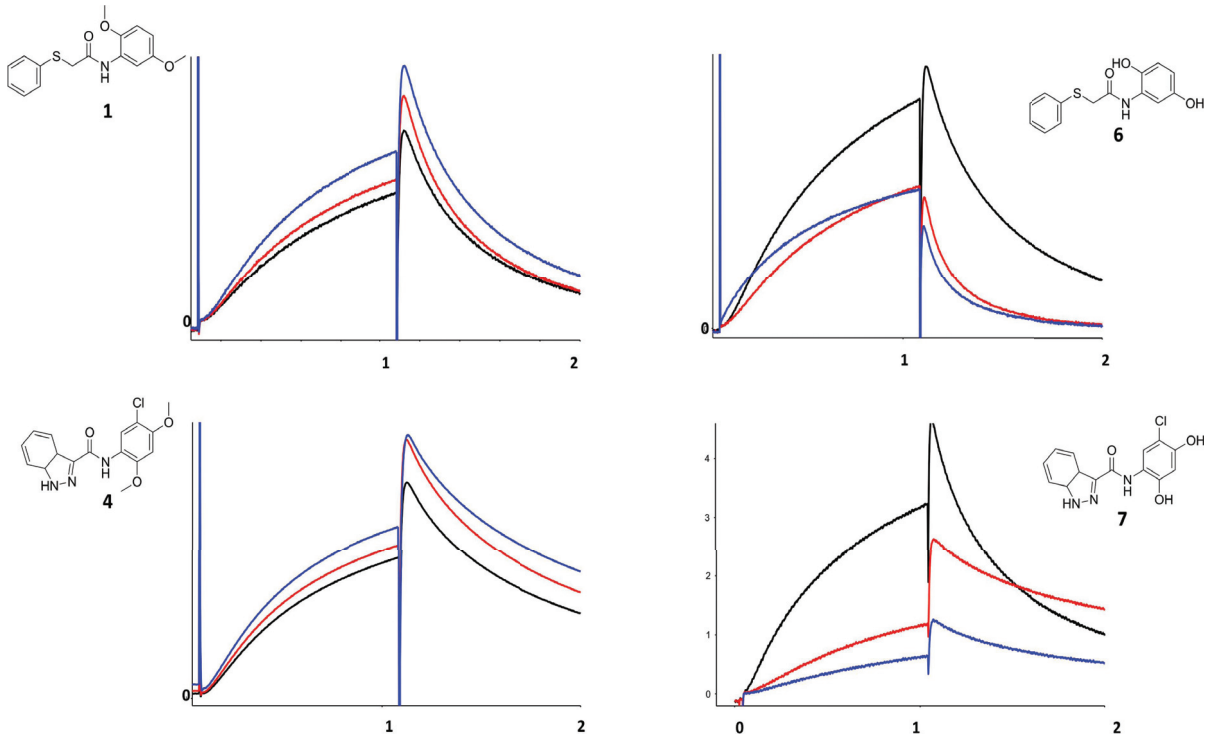

Fig. (3). HERG current traces recorded under the control conditions (black), during the exposure to the specified molecules and after washout of the molecules (blue). In all cases, the following voltage clamp protocol was used: holding voltage -80 mV, currents elicited by 1-s depolarizing pulses to +20 mV once every 60 s, and tail currents were recorded at -60 mV. The current amplitude increased slightly after washing out of the molecules **1** and **4**: this could be due to mixed activator/inhibitor effects, and the latter was reversed more readily than the former. On the other hand, compounds **6** and **7** were clearly hERG inhibitors, with varying degree of reversibility after washing out of the molecules.

bearing heterocycles or groups present in other top-ranked molecules from the LBVS outcome. On the other side, despite their poor solubility, **1** and **4** showed a moderate enhancing effect, therefore we investigated the possibility to improve their activity by synthesizing the dihydroxy-analogs **6** and **7**, respectively. On the same line, we decided to study the role of methoxy *vs* hydroxy groups also in the SAR on **3**. The synthetic route to obtain the desired compounds allowed the reactions to be conducted in a parallel fashion. Amides **1**, **4**, **8-12** were synthesized through a DCC-HOBt mediated coupling employing carboxylic acids **17-21** and amines **22-24**, then treating with boron tribromide to afford the hydroxyl derivatives **6**, **7**, **13-16** (Scheme **1**). All the newly synthesized compounds (**6-17**) were then tested for their ability to modulate the hERG activation (Table **3**).

Even though the di-hydroxy amides **6** and **7** were found to be more soluble than the parent compounds, a controversial result was obtained in the electrophysiology assays shown in Fig. (**3**). Indeed, rather than acting as hERG activators, they turned out to be currents suppressors. Albeit disappointing, this finding was not completely unexpected, as even the reference compound NS1643 shows a blocking behavior at high concentrations [20]. Since the blockers binding site is known to be highly unspecific in terms of molecular determinants, it is possible that many hERG enhancers can bind to multiple sites, and that the net effect on the channel kinetics is the result of a subtle concentration-depending balance of the affinities to each site. Such a scenario has also been supported by the theoretical and experimental results reported by Durdagi *et al*., which rationalized the dual pharmacological behavior of NS1643 by the presence of multiple spatially separated binding sites mediating different modulating effects [23]. Interestingly, going from **7** to **9**, thus maintaining the indazole fragment but coupling it with the 2-methoxy-5-(*tert*-butyl)-aniline, once again a reversed pharmacological activity was observed, since **9** showed a slight enhancing effect on current amplitude (134%, see Table **3** and Fig. **4**), while a drop of activity was observed with its hydroxy analog **14**, confirming the complexity of the protein-ligand interaction in hERG.

Among the methoxy amide **8-12** derivatives, also compound **10** (Table **3**, Fig. **4**), which is the methoxy analog of **3**, showed a modest activating effect (160%) on hERG, suggesting that the 2 Br-phenyl portion could play an important role. However, compared to parent compound **3**, a loss of activity was detected. Concerning the hydroxyl derivatives **13-16**, surprisingly none was able to show an enhancing activity.

Taken together, these results revealed the hydroxyl function in the *ortho* position not to be an essential requirement to obtain an effective modulation of the hERG channel. Moreover, the amide linkage proved to be a valid and synthetically accessible bioisosteric replacement of the urea in the search of novel hERG activators.

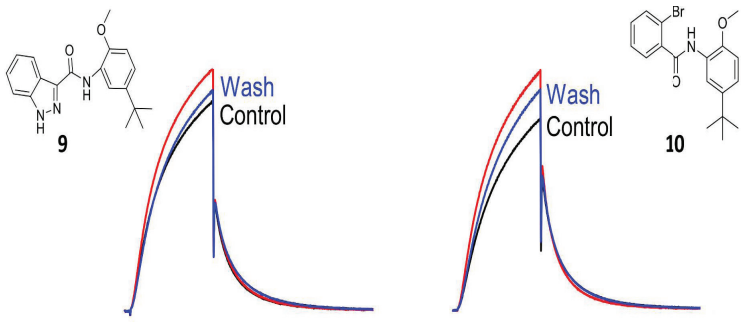

Fig. (4). HERG current traces recorded under the control conditions (black), during the exposure to the specified molecules and concentrations (red) and after washout of the molecules (blue). The voltage clamp protocol was the same as described for Fig. (**3**).

CONCLUSION

The hERG potassium channel has long been known as an antitarget in drug discovery, because its undesired block promotes the prolongation of the plateau phase of the action potential in myocytes leading to potentially serious cardiac conditions. Since the discovery of molecules able to modulate positively the IKr currents, however, the paradigm of the hERG pharmacology has changed. Indeed, the binding of small molecules to the channel is no longer necessarily perceived as an unwanted event, as drugs able to activate the channel could in principle be exploited for their potential therapeutic effects. Unfortunately, the advancements in this field of drug discovery is strongly slowed down by difficulties due both to the lack of the hERG crystal structure and to the uncertainties related to the location of the binding site of activators. Rather than pursuing a problematic structure-based strategy, in this study, we took advantage of a ligand-based approach to identify new compounds as hERG activators by means of a virtual screening campaign. One of the selected hits among the final library proved to enhance hERG current of 195%, confirming that our protocol was successful in providing a new and accessible scaffold worth to be explored by combinatorial synthetic strategies.

CONFLICT OF INTEREST

The authors confirm that this article content has no conflict of interest.

ACKNOWLEDGEMENTS

The authors thank Andrea Sartini for technical assistance, and also acknowledge funding from Istituto Italiano di Tecnologia, Genova, Italy (Seed project: HERGSYM).

REFERENCES

[1] Bagal, S.K.; Brown, A.D.; Cox, P.J.; Omoto, K.; Owen, R.M.; Pryde, D.C.; Sidders, B.; Skerratt, S.E.; Stevens, E.B.; Storer, R.I.; Swain, N. a. Ion channels as therapeutic targets: a drug discovery perspective. *J. Med. Chem.*, **2013**, *56*, 593-624.

[2] Gamper, N. Osmosensitivity through the PIP2 Availability: Just Add Water. *J. Physiol.*, **2010**, *588*, 3631-3632.

[3] Hubner, C.A. Ion Channel Diseases. *Hum. Mol. Genet.*, **2002**, *11*, 2435-2445.

[4] Perry, M.; Sanguinetti, M.; Mitcheson, J. Revealing the structural basis of action of hERG potassium channel activators and blockers. *J. Physiol.*, **2010**, *588*, 3157-3167.

[5] Zhou, P.; Babcock, J.; Liu, L.; Li, M.; Gao, Z. Activation of Human Ether-a-Go-Go Related Gene (hERG) Potassium Channels by Small Molecules. *Acta Pharmacol. Sin.*, **2011**, *32*, 781-788.

[6] He, F.-Z.; McLeod, H.L.; Zhang, W. Current Pharmacogenomic Studies on hERG Potassium Channels. *Trends Mol. Med.*, **2013**, *19*, 227-238.

[7] Xu, X.; Recanatini, M.; Roberti, M.; Tseng, G. Probing the Binding Sites and Mechanisms of Action of Two Human Ether-a-Go-Go-Related Gene Channel Activators, 1,3-Bis-(2-Hydroxy-5-Trifluoromethyl-Phenyl)-Urea (NS1643) and 2-[2-(3,4-Dichloro-Phenyl)-2,3-Dihydro-1H-Isoindol-5-Ylamino]-Nicotinic Acid (PD3). *Mol. Pharmacol.*, **2008**, *73*, 1709-1721.

[8] Di Martino, G.P.; Masetti, M.; Ceccarini, L.; Cavalli, A.; Recanatini, M. An automated docking protocol for herg channel blockers. *J. Chem. Inf. Model.*, **2013**, *53*, 159-175.

[9] Perrin, M.J.; Subbiah, R.N.; Vandenberg, J.I.; Hill, A.P. Human Ether-a-Go-Go Related Gene (hERG) K+ channels: function and dysfunction. *Prog. Biophys. Mol. Biol.*, **2010**, *98*, 137-148.

[10] Trudeau, M.; Warmke, J.; Ganetzky, B.; Robertson, G. HERG, a human inward rectifier in the voltage-gated potassium channel family. *Science.*, **1995**, *269*, 92-95.

[11] Babcock, J.J.; Li, M. hERG Channel Function: Beyond Long QT. *Acta Pharmacol. Sin.*, **2013**, *34*, 329-335.

[12] Recanatini, M.; Poluzzi, E.; Masetti, M.; Cavalli, A.; De Ponti, F. QT Prolongation through hERG K(+) channel blockade: current knowledge and strategies for the early prediction during drug development. *Med. Res. Rev.*, **2005**, *25*, 133-166.

[13] Kim, P.Y.; Ewer, M.S. Chemotherapy and QT prolongation: overview with clinical perspective. *Curr. Treat. Options Cardiovasc. Med.*, **2014**, *16*, 303.

[14] Sanguinetti, M.C.; Tristani-Firouzi, M. hERG potassium channels and cardiac arrhythmia. *Nature*, **2006**, *440*, 463-469.

[15] Cavalli, A.; Buonfiglio, R.; Ianni, C.; Masetti, M.; Ceccarini, L.; Caves, R.; Chang, M.W.Y.; Mitcheson, J.S.; Roberti, M.; Recanatini, M. Computational Design and Discovery of "Minimally Structured" hERG Blockers. *J. Med. Chem.*, **2012**, *55*, 4010-4014.

[16] Wang, S.; Li, Y.; Xu, L.; Li, D.; Hou, T. Recent developments in computational prediction of hERG blockage. *Curr. Top. Med. Chem.*, **2013**, *13*, 1317-1326.

[17] Raschi, E.; Vasina, V.; Poluzzi, E.; De Ponti, F. The hERG K+ channel: target and antitarget strategies in drug development. *Pharmacol. Res.*, **2008**, *57*, 181-195.

[18] Zhang, H.; Zou, B.; Yu, H.; Moretti, A.; Wang, X.; Yan, W.; Babcock, J.J.; Bellin, M.; McManus, O.B.; Tomaselli, G.; Nan, F.; Laugwitz, K.-L.; Li, M. Modulation of hERG potassium channel gating normalizes action potential duration prolonged by dysfunctional KCNQ1 potassium channel. *Proc. Natl. Acad. Sci. USA*, **2012**, *109*, 11866-11871.

[19] Hansen, R.S.; Diness, T.G.; Christ, T.; Demnitz, J.; Ravens, U.; Olesen, S.; Grunnet, M. Activation of Human Ether-a-Go-Go-Related Gene Potassium Channels by the Diphenylurea 1,3-Bis-(2-Hydroxy-5-Trifluoromethyl-Phenyl)-Urea (NS1643). *Mol. Pharmacol.*, **2006**, *69*, 266-277.

[20] Casis, O.; Olesen, S.; Sanguinetti, M.C. Mechanism of Action of a novel human ether-a-go-go-related gene channel activator. *Mol. Pharmacol.*, **2006**, *69*, 658-665.

[21] Szabó, G.; Farkas, V.; Grunnet, M.; Mohácsi, a; Nánási, P.P. Enhanced repolarization capacity: new potential antiarrhythmic strategy based on HERG channel activation. *Curr. Med. Chem.*, **2011**, *18*, 3607-3621.

[22] Hansen, R.S.; Diness, T.G.; Christ, T.; Wettwer, E.; Ravens, U.; Olesen, S.; Grunnet, M. Biophysical characterization of the new human ether-a-go-go-related gene channel opener NS3623 [N-(4-Bromo-2-(1H-Tetrazol-5-Yl)-Phenyl)-N'-(3'-Trifluoromethylphenyl)urea]. *Mol. Pharmacol.*, **2006**, *70*, 1319-1329.

[23] Durdagi, S.; Guo, J.; Lees-Miller, J.P.; Noskov, S.Y.; Duff, H.J. Structure-guided topographic mapping and mutagenesis to elucidate binding sites for the human ether-a-go-go-related gene 1 potassium channel (KCNH2) activator NS1643. *J. Pharmacol. Exp. Ther.*, **2012**, *342*, 441-452.

[24] http://www.enamine.net/.

[25] OEChem, version 1.7.7, OpenEye Scientific Software, Inc., Santa Fe, NM, U. www.eyesopen.com.

[26] Kirchmair, J.; Distinto, S.; Markt, P.; Schuster, D.; Spitzer, G.M.; Liedl, K.R.; Wolber, G. How to optimize shape-based virtual screening: choosing the right query and including chemical information. *J. Chem. Inf. Model.*, **2009**, *49*, 678-692.

[27] Frisch, M. J.; Trucks, G. W.; Schlegel, H. B.; Scuseria, G. E.; Robb, M. A.; Cheeseman, J. R.; Montgomery, J. A. Jr.; Vreven, T.; Kudin, K. N.; Burant, J. C.; Millam, J. M.; Iyengar, S. S.; Tomasi, J.; Barone, V.; Mennucci, B.; Cossi, M.; Scalmani, G.; Rega, N.; Petersson, G. A.; Nakatsuji, H.; Hada, M.; Ehara, M.; Toyota, K.; Fukuda, R.; Hasegawa, J.; Ishida, M.; Nakajima, T.; Honda, Y.; Kitao, O.; Nakai, H.; Klene, M.; Li, X.; Knox, J. E.; Hratchian, H. P.; Cross, J. B.; Bakken, V.; Adamo, C.; Jaramillo, J.; Gomperts, R.; Stratmann, R. E.; Yazyev, O.; Austin, A. J.; Cammi, R.; Pomelli, C.; Ochterski, J. W.; Ayala, P. Y.; Morokuma, K.; Voth, G. A.; Salvador, P.; Dannenberg, J. J.; Zakrzewski, V. G.; Dapprich, S.; Daniels, A. D.; Strain, M. C.; Farkas, O.; Malick, D. K.; Rabuck, A. D.; Raghavachari, K.; Foresman, J. B.; Ortiz, J. V.; Cui, Q.; Baboul, A. G.; Clifford, S.; Cioslowski, J.; Stefanov, B. B.; Liu, G.; Liashenko, A.; Piskorz, P. Komaromi, I.; Martin, R. L.; Fox, D. J.; Keith, T.; Al-Laham, M. A.; Peng, C. Y.; Nanayakkara, A.; Challacombe, M.; Gill, P. M. W.; Johnson, B.; Chen, W.; Wong, M. W.; Gonzalez, C.; Pople, J. A. Gaussian 03, Revision C.02. (2004) Wallingford CT, Gaussian, I.

[28] Irwin, J.J.; Sterling, T.; Mysinger, M.M.; Bolstad, E.S.; Coleman, R.G. ZINC: a free tool to discover chemistry for biology. *J. Chem. Inf. Model.*, **2012**, *52*, 1757-1768.

[29] FILTER, version 2.02, OpenEye Scientific Santa Fe, NM, USA. www.eyesopen.com.

[30] Wang, R.; Fu, Y.; Lai, L. A new atom-additive method for calculating partition coefficients. *J. Chem. Inf. Model.*, **1997**, *37*, 615-621.

[31] Kirchmair, J.; Wolber, G.; Laggner, C.; Langer, T. Comparative performance assessment of the conformational model generators omega and catalyst: a large-scale survey on the retrieval of protein-bound ligand conformations. *J. Chem. Inf. Model.*, **2006**, *46*, 1848-1861.

[32] Quevedo, M.A.; Ribone, S.R.; Briñón, M.C.; Dehaen, W. Development of a receptor model for efficient in silico screening of HIV-1 integrase inhibitors. *J. Mol. Graph. Model.*, **2014**, *52*, 82-90.

[33] Avram, S.I.; Pacureanu, L.M.; Bora, A.; Crisan, L.; Avram, S.; Kurunczi, L. ColBioS-FlavRC: A Collection of Bioselective Flavonoids and Related Compounds Filtered from High-Throughput Screening Outcomes. *J. Chem. Inf. Model.*, **2014**, *54*, 2360-2370.

[34] Hamza, A.; Wei, N.-N.; Zhan, C.-G. Ligand-based virtual screening approach using a new scoring function. *J. Chem. Inf. Model.*, **2012**, *52*, 963-974.

[35] ROCS 3.2.0.4: OpenEye Scientific Software, Santa Fe, N. http://www.eyesopen.com.

[36] Hawkins, P.C.D.; Skillman, a G.; Nicholls, A. Comparison of shape-matching and docking as virtual screening tools. *J. Med. Chem.*, **2007**, *50*, 74-82.

[37] EON 2.2.0.5: OpenEye Scientific Software, Santa Fe, N. http://www.eyesopen.com.

[38] Halgren, T.A. Merck Molecular Force Field. I. Basis, Form, Scope, Parameterization, and Performance of MMFF94. *J. Comput. Chem.*, **1996**, *17*, 490-519.

[39] Bayly, C.I.; Cieplak, P.; Cornell, W.; Kollman, P.A. A well-behaved electrostatic potential based method using charge restraints for deriving atomic charges: the RESP model. *J. Phys. Chem.*, **1993**, *97*, 10269-10280.

[40] Cornell, W.D.; Cieplak, P.; Bayly, C.I.; Kollmann, P.A. Application of RESP charges to calculate conformational energies, hydrogen bond energies, and free energies of solvation. *J. Am. Chem. Soc.*, **1993**, *115*, 9620-9631.

[41] Abagyan, R.; Totrov, M.; Kuznetsov, D. ICM?A New method for protein modeling and design: applications to docking and structure prediction from the distorted native conformation. *J. Comput. Chem.*, **1994**, *15*, 488-506.

[42] Michener, C.D.; Sokal, R.R. A Quantitative Approach to a Problem in Classification. *Evolution (N. Y).*, **1957**, *11*, 130.

[43] Masetti, M.; Cavalli, A.; Recanatini, M. Modeling the hERG potassium channel in a phospholipid bilayer: molecular dynamics and drug docking studies. *J. Comput. Chem.*, **2008**, *29*, 795-808.

[44] Tseng, G.-N.; Sonawane, K.D.; Korolkova, Y. V; Zhang, M.; Liu, J.; Grishin, E. V; Guy, H.R. Probing the outer mouth structure of the HERG channel with peptide toxin footprinting and molecular modeling. *Biophys. J.*, **2007**, *92*, 3524-3540.

Received: July 23, 2014 **Revised: October 8, 2014** **Accepted: November 10, 2014**